

Prototypical Prompting for Text-to-image Person Re-identification

Shuanglin Yan
Nanjing University of Science and
Technology
Nanjing, China
shuangliny@njust.edu.cn

Jun Liu
Lancaster University
Lancaster, United Kingdom
j.liu81@lancaster.ac.uk

Neng Dong
Nanjing University of Science and
Technology
Nanjing, China
neng.dong@njust.edu.cn

Liyan Zhang*
Nanjing University of Aeronautics
and Astronautics
Nanjing, China
zhangliyan@nuaa.edu.cn

Jinhui Tang
Nanjing University of Science and
Technology
Nanjing, China
jinhuitang@njust.edu.cn

ABSTRACT

In this paper, we study the problem of Text-to-Image Person Re-identification (TIREID), which aims to find images of the same identity described by a text sentence from a pool of candidate images. Benefiting from Vision-Language Pre-training, such as CLIP (Contrastive Language-Image Pretraining), the TIREID techniques have achieved remarkable progress recently. However, most existing methods only focus on instance-level matching and ignore identity-level matching, which involves associating multiple images and texts belonging to the same person. In this paper, we propose a novel prototypical prompting framework (Propot) designed to simultaneously model instance-level and identity-level matching for TIREID. Our Propot transforms the identity-level matching problem into a prototype learning problem, aiming to learn identity-enriched prototypes. Specifically, Propot works by ‘initialize, adapt, enrich, then aggregate’. We first use CLIP to generate high-quality initial prototypes. Then, we propose a domain-conditional prototypical prompting (DPP) module to adapt the prototypes to the TIREID task using task-related information. Further, we propose an instance-conditional prototypical prompting (IPP) module to update prototypes conditioned on intra-modal and inter-modal instances to ensure prototype diversity. Finally, we design an adaptive prototype aggregation module to aggregate these prototypes, generating final identity-enriched prototypes. With identity-enriched prototypes, we diffuse its rich identity information to instances through prototype-to-instance contrastive loss to facilitate identity-level matching. Extensive experiments conducted on three benchmarks demonstrate the superiority of Propot compared to existing TIREID methods.

*Corresponding author.

Permission to make digital or hard copies of all or part of this work for personal or classroom use is granted without fee provided that copies are not made or distributed for profit or commercial advantage and that copies bear this notice and the full citation on the first page. Copyrights for components of this work owned by others than the author(s) must be honored. Abstracting with credit is permitted. To copy otherwise, to republish, to post on servers or to redistribute to lists, requires prior specific permission and/or a fee. Request permissions from permissions@acm.org.

MM '24, October 28-November 1, 2024, Melbourne, VIC, Australia.

© 2024 Copyright held by the owner/author(s). Publication rights licensed to ACM.

ACM ISBN 979-8-4007-0686-8/24/10

<https://doi.org/10.1145/3664647.3681165>

CCS CONCEPTS

• **Computing methodologies** → **Visual content-based indexing and retrieval.**

KEYWORDS

Text-to-image person re-identification; Identity-level matching; Prototypical prompting

ACM Reference Format:

Shuanglin Yan, Jun Liu, Neng Dong, Liyan Zhang, and Jinhui Tang. 2024. Prototypical Prompting for Text-to-image Person Re-identification. In *Proceedings of the 32nd ACM International Conference on Multimedia (MM '24)*, October 28-November 1, 2024, Melbourne, VIC, Australia. ACM, New York, NY, USA, 10 pages. <https://doi.org/10.1145/3664647.3681165>

1 INTRODUCTION

Person re-identification (ReID), devoted to searching a person-of-interest across different times, locations, and camera views, has garnered increasing interest due to its huge practicality. In recent years, we have witnessed great progress on image-to-image person re-identification (IIReID) [10, 11, 25, 30, 31, 70], which has been successfully applied in various practical scenarios. However, ReID is still challenging when pedestrian images from some cameras are missing. In contrast, textual descriptions are more readily accessible and freer than images collected by specialized equipment, which can be obtained from witnesses at the scene. Thus, text-to-image person re-identification (TIREID) [33] has received a lot of research attention recently owing to it being closer to real-world scenarios.

Compared to IIReID, TIREID faces a significant challenge in bridging the modal gap between images and texts while modeling their correspondence. Various methods have been devised to address this challenge by cross-modal interactive attention mechanisms [45, 77, 80], semantically aligned local feature learning [6, 9, 49, 69], and fine-grained auxiliary task-enhanced global feature learning [43, 44]. Nowadays, the emergence of vision-language pre-training models (VLP) has propelled the advancements in computer vision, showcasing exceptional capabilities in semantic understanding and multi-modal alignment. It is intuitive to consider that the rich multi-modal prior information of VLP can be harnessed to enhance TIREID models in modeling inter-modal correspondence.

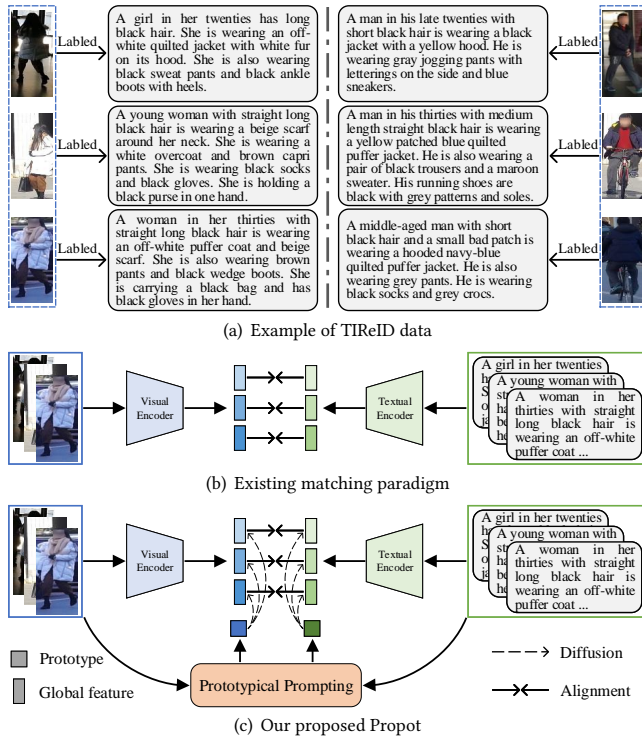


Figure 1: The motivation of Propot. (a) Instances under the same identity show significant differences. (b) Current TIReID methods only focus on instance-level matching and ignore identity-level matching. (c) Our Propot proposes a prototype prompting framework to create identity-enriched prototypes and diffuse their rich identity information to instances for modeling identity-level matching.

Some follow-up CFine [68], IRRa [21], and RaSa [72] extend VLP for TIReID, greatly promoting the progress of this task.

Despite the success of VLP-based methods, the performance of TIReID still lags behind that of IIReID, especially in complex scenes like multiple cameras and drastic view variation. This is primarily due to the specificity of the TIReID task. As shown in Figure 1(a), there are multiple images of the same identity, each annotated with specific text at the instance level. The goal of TIReID is to match all images of the same identity given a text, meaning to correctly associate each text with all images of the same identity. However, most existing methods, constrained by the alignment objective function [67], only consider **instance-level matching** between each image and its annotated text, ignoring matches with other non-annotated texts of the same identity, called **identity-level matching**. An intuitive idea to this problem is to directly match all images and texts under the same identity, but this can disrupt instance-level matching relationship [67] due to huge view variations, leading to performance collapse. In this paper, we thus ask: *Can an end-to-end efficient TIReID model be trained to simultaneously model instance-level and identity-level matching?*

To address this problem, we propose a novel **Prototypical prompting framework (Propot)** that enables the network to model instance-level and identity-level matching for TIReID simultaneously. As

shown in Figure 1, existing TIReID methods only model instance-level matching between each image and its labeled text. In contrast, our Propot further introduces identity-level matching based on instance-level matching. We learn a prototype containing rich identity information for each identity and diffuse the rich information from the prototype to each instance, indirectly modeling identity-level matching. This transforms the identity-level matching problem into an **identity-enriched prototype learning** problem.

Specifically, our Propot follows the ‘initialize, adapt, enrich, then aggregate’ pipeline. Initially, we leverage CLIP’s strong multi-modal alignment capability to cluster instance (image/text) features under each identity, forming the initial prototype for each identity. Since there’s a gap between CLIP and TIReID data, this prototype is not fully adapted to TIReID. To address this, we propose a domain-conditional prototypical prompting (DPP) module, which introduces a set of learnable prompt tokens to learn target domain knowledge and adapt the initial prototype to the TIReID task. However, instances under the same identity exhibit significant diversity due to factors like view changes and camera parameters. Ignoring this diversity can lead to a monotonous prototype, losing rich identity information. Thus, we propose an instance-condition prototypical prompting (IPP) module. This module generates two prototypical prompts conditioned on a batch of instances, leveraging both intra-modal and inter-modal instances to enhance diversity and bridge the modal gap. To integrate the multiple prototypes generated above, an adaptive prototype aggregation (APA) module is designed, which treats the initial CLIP-generated prototype as the baseline and adaptively ensemble these prototypes as the final prototype. Finally, we utilize a prototype-to-instance contrastive loss to diffuse the prototype’s rich identity information to each instance, enabling effective modeling of identity-level matching. Propot is single-stage and end-to-end trainable. During inference, only the backbone network is used, which is simple and efficient.

Here are the main contributions of our paper: (1) We propose an end-to-end trainable prototypical prompting framework to model instance-level and identity-level matching for TIReID simultaneously. (2) We transform the identity-level matching problem into an identity-enriched prototype learning problem, and introduce a novel ‘initialize, adapt, enrich, then aggregate’ prototype learning scheme. (3) Extensive experiments verify the effectiveness of Propot and achieve superior performance on three benchmarks.

2 RELATED WORK

2.1 Text-to-Image Person Re-identification

TIReID [33] has gained significant attention in recent years. Existing studies can be broadly divided into the following categories: better model architectures and optimization losses, better alignment strategies, and richer prior information. Previous methods [4, 75, 78] have focused on designing network and optimization loss to learn globally aligned features in a joint embedding space. These methods are simple and efficient, but ignore fine-grained correspondence [47, 53–55]. To address these limitations, subsequent methods have refined matching strategies to mine fine-grained correspondence between modalities. Some methods [23, 33, 45, 57, 77, 80] have emerged to achieve fine-grained matching through interactions between local parts of images and texts. While effective, these approaches require

significant computational resources. To mitigate computational overhead, other works [6, 9, 63] adopt local image parts to guide the generation of locally aligned text features, avoiding pairwise interactions. However, the effectiveness of these methods depends on the quality of explicitly acquired local parts. As an alternative, diverse aggregation schemes [29, 49, 69] have been proposed to adaptively aggregate images and texts into modality-shared local features, avoiding explicit local part acquisition.

Recently, vision-language pre-training models (VLP) [48] have made significant progress. To leverage their rich multi-modal knowledge, recent methods [1, 16, 21, 46, 68] have proposed diverse strategies to tailor VLP for TIReID, resulting in notable performance enhancements. However, existing methods often overlook the specific nature of TIReID as a challenge involving matching multi-view image-text pairs at the identity level, rather than merely at the instance level. Addressing this concern, several methods [9, 67, 72] have been proposed. SSAN [9] introduces an enhanced alignment loss to simultaneously align the image with its annotated text and another text sharing the same identity. LCR²S [67] designs a teacher-student network architecture to randomly fuse two images/texts under the same identity and then align them to model identity-level matching. RaSa [72] introduces an additional memory bank to store more samples, indirectly expanding the batch size to model many-to-many matching. These approaches yielded notable performance gains, it had limitations in fully integrating multi-view information and exhibited lower training efficiency. In this study, we present an end-to-end framework to learn a prototype with comprehensive information for each identity using the training set, and transfer multi-view information to individual samples for identity-level matching. This approach enhances both efficiency and the integration of multi-view data for TIReID.

2.2 Vision-Language Pre-Training

Nowadays, the "pre-training and fine-tuning" paradigm stands as a foundational approach in the computer vision community, in which pre-training models that can provide rich prior knowledge for various downstream vision tasks have gained increasing attention. Previous prevailing practice is rooted in the supervised unimodal pre-training [12, 17] on ImageNet [7]. However, to improve representation capabilities and overcome annotation constraints, a new paradigm called language-supervised vision pre-training (vision-language pre-training, VLP) has emerged. Within VLP, investigating the interaction between vision and language has become a central research focus. Several works [5, 27, 28, 37, 60] have been proposed to model the interaction of vision and language based on some multi-modal reasoning tasks, such as masked language/region modeling, and image captioning [40]. Recently, contrastive representation learning [20, 42, 48, 73] has gained attention, which learns representations by contrasting positive pairs against negative pairs. The representative work, Contrastive Language-Image Pretraining (CLIP) [48], has strong multi-modal semantic representation and zero-shot generalization capabilities, which is trained on 400 million image-text pairs. CLIP has shown promising adaptability for various downstream tasks like video-text retrieval [13, 38], referring image segmentation [61], action recognition [65, 66], and

person re-identification [68]. Our work builds upon CLIP and utilizes its ample multi-modal knowledge to learn identity-enriched prototypes.

2.3 Prompt Learning

Prompt learning [22, 51], originating from natural language processing (NLP), is a method used to customize pre-training models for different tasks by providing instructions in the form of sentences, known as prompts. Early prompts were manually designed for specific tasks, but recent studies have introduced prompt learning, where task-specific prompts are automatically generated during fine-tuning. This approach addresses issues like instability and knowledge bias. Prompt learning has now been extended to computer vision. CoOp [79] pioneered the application of prompt learning to adapt large vision-language models in computer vision, while CoCoOp [56] built upon CoOp to introduce a conditional prompt learning framework, improving generalization. Chen et al. [24] proposed efficiently adapting the CLIP model to the video understanding task by optimizing a few continuous prompt vectors. CLIP-ReID [32] designed a two-stage framework to generate coarse descriptions of pedestrians, leveraging CLIP's capabilities for ReID. Inspired by these, in this work we propose using prompt learning to learn comprehensive prototype representations to model identity-level matching for TIReID.

3 THE PROPOT FRAMEWORK

Our Propot is a conceptually simple end-to-end trainable framework, and the overview is depicted in Figure 2. We first extract features of images and texts through visual and textual encoders, followed by instance-level and identity-level matching.

3.1 Feature Extraction

To harness the vast multi-modal knowledge in CLIP, we leverage its image and text encoders to initialize Propot's image and text backbones. Concretely, for an image-text pair (I, T) , we exploit CLIP pre-trained ViT model to extract visual representations for the image I , resulting in the global visual feature $v \in \mathbb{R}^d$. For the text caption T , the CLIP's textual encoder is utilized to generate the global textual feature $t \in \mathbb{R}^d$.

Instance-level matching involves directly aligning v with t . For identity-level matching, we transform it into an identity-enriched prototype learning problem. The aim is to learn a rich prototype containing all instance identity information for each identity in the training set. In Propot, the prototype learning method is crucial. While it is conceivable to learn a prototype for each identity from scratch, akin to previous method [32], such an approach can encounter challenges in network convergence and may not ensure prototype quality. To address these concerns, we introduce a novel 'initialize, adapt, enrich, then aggregate' prototype learning scheme, detailed in the subsequent subsections.

3.2 Initial Prototype Generation

We start by utilizing the CLIP model to extract features for each instance in the TIReID training set, leveraging its strong semantic information extraction and multi-modal alignment capabilities. We then cluster these instance features based on shared identity labels to produce initial prototypes for each modality. Specifically, given

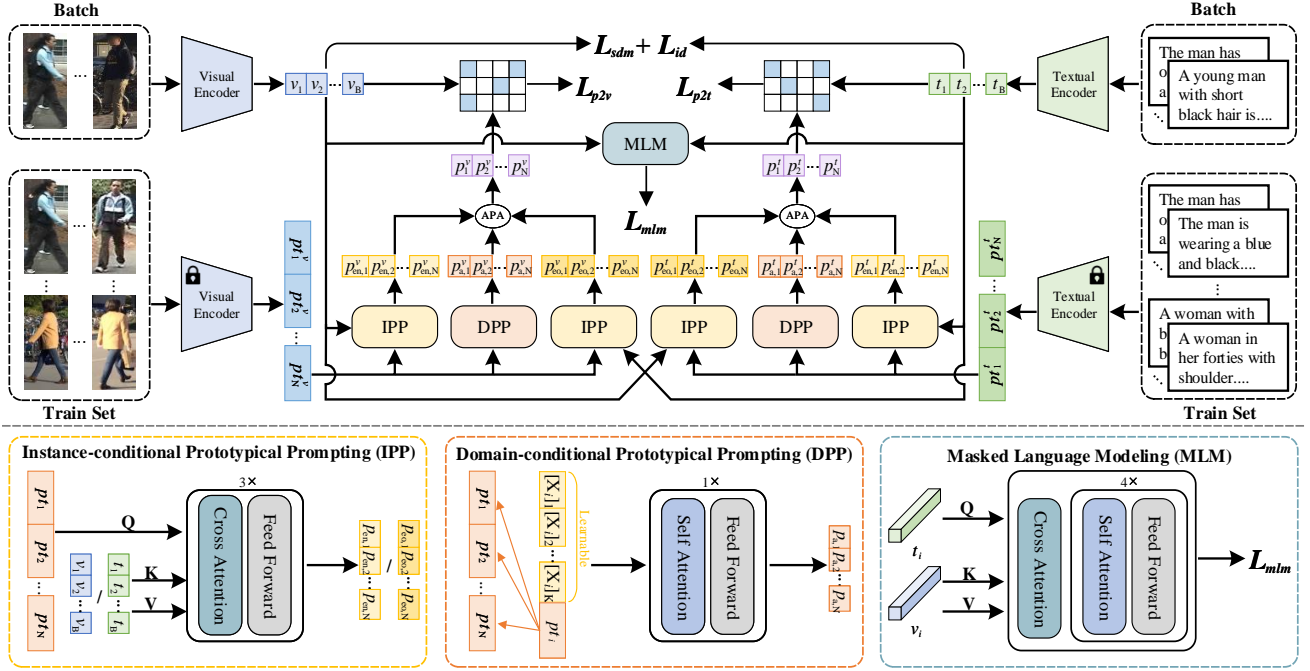


Figure 2: Overview of our Propot. It includes instance-level matching and identity-enriched prototype learning. For instance-level matching, each image and its annotated text are directly aligned through SDM loss (Baseline). For prototype learning, we first utilize pre-trained CLIP to generate initial prototypes (pt^v and pt^t). We then adapt the initial prototypes to TIReID through the DPP module, resulting in task-adapted prototypes (p_a^v and p_a^t). The IPP module updates the prototypes conditioned on a batch of intra-modal and inter-modal instances, generating intra-modal and inter-modal enriched prototypes (p_{en}^v , p_{en}^t , p_{eo}^v and p_{eo}^t). The multiple prototypes are aggregated using Adaptive Prototypical Aggregation (APA) to generate final prototypes (p^v and p^t). Their rich identity information is then diffused to each instance using prototype-to-instance contrastive loss (\mathcal{L}_{p2v} , \mathcal{L}_{p2t}) to model identity-level matching. Moreover, we introduce the MLM module to enhance fine-grained matching. During testing, only visual and textual encoders are used for inference.

the training set $\{I_i, T_i, Y_i\}_{i=1}^{N_s}$, where $Y_i \in \{L_1, L_2, \dots, L_N\}$ represents the identity label, N_s denotes the number of pairs, and N denotes the number of identity label, we employ the pre-trained CLIP visual and textual encoders to obtain the visual and textual features $\{v_i, t_i\}_{i=1}^{N_s}$ of all image-text pairs. We then perform feature clusters on the image and text features. Taking identity L_i as an example, We generate initial prototypes pt_i^v and pt_i^t for identity L_i as follows:

$$pt_i^v = \sum_{j=1, Y_j \in L_i}^{N_i} v_j, \quad pt_i^t = \sum_{j=1, Y_j \in L_i}^{N_i} t_j, \quad (1)$$

where N_i denotes the number of instances under the identity L_i . Therefore, for the entire training set, we can generate visual and textual initial prototype sets $pt^v = [pt_1^v, pt_2^v, \dots, pt_N^v] \in \mathbb{R}^{N \times d}$ and $pt^t = [pt_1^t, pt_2^t, \dots, pt_N^t] \in \mathbb{R}^{N \times d}$.

3.3 Domain-conditional Prototypical Prompting

Benefiting from CLIP’s powerful capabilities, the initial prototype effectively captures some identity information to model identity-level matching, leading to improved performance (as shown in Table 4), which confirms the validity of our idea. However, a notable challenge arises due to the domain gap between the pre-training data of CLIP and the TIReID dataset. Consequently, the

identity information mined by CLIP’s features falls short, significantly diminishing the impact of the initial prototype. To address this challenge, inspired by the Contextual Optimization (CoOp) framework [79], which introduces learnable context vectors to adapt VLP to downstream tasks, we introduce a Domain-conditional Prototypical Prompting (DPP) module to adjust the initial prototype to the TIReID task. Specifically, we add a set of learnable contextual prompt vectors before each initial prototype. These vectors undergo training on the TIReID dataset concurrently with the network, gaining domain knowledge specific to the TIReID task. These vectors then transmit the domain knowledge to each initial prototype through the self-attention encoder (SAE), aiding in the adaptation of prototypes to the TIReID task.

Formally, for each initial prototype pt_i , we add a set of learnable contextual prompt vectors $\{[X_i]_1, [X_i]_2, \dots, [X_i]_K\} \in \mathbb{R}^{K \times d}$ before it, where $[X_i]$ is the visual contextual prompt vector $c_{v,i}$ for the visual prototype pt_i^v , and $[X_i]$ is the textual contextual prompt vector $c_{t,i}$ for the textual prototype pt_i^t . Then, we feed $\{[X_i]_1, [X_i]_2, \dots, [X_i]_K, pt_i\} \in \mathbb{R}^{(K+1) \times d}$ into SAE to pass the information to the initial prototype for updating it.

$$P_{a,i} = SAE(\{[X_i]_1, [X_i]_2, \dots, [X_i]_K, pt_i\}), \quad (2)$$

where $P_{a,i} \in \mathbb{R}^{(K+1) \times d}$, and $p_{a,i} = P_{a,i}[-1] \in \mathbb{R}^d$ represents the task-adaptive prototype. SAE is comprised of N_a blocks, with each block containing a multi-head self-attention layer and a feed-forward network layer. The above process allows us to generate modality-specific task-adaptive prototypes, $p_{a,i}^v$ and $p_{a,i}^t$, for the input prototypes of different modalities.

3.4 Instance-conditional Prototypical Prompting

So far, we have generated a prototype adapted to the TIReID task. However, as depicted in Figure 1, instances of the same identity showcase notable diversity due to factors like view changes and camera parameters. The previously derived prototype fails to account for this diversity, resulting in the loss of some discriminative identity information. To solve this problem, inspired by Conditional Context Optimization (CoCoOp) [56], we propose an Instance-conditional Prototypical Prompting (IPP) module. This module updates the prototype conditioned on each batch of the input instances, enabling the comprehensive mining of instance-specific information and ensuring diversity within the prototype.

Specifically, for a batch of B image-text pairs $\{I_i, T_i\}_{i=1}^B$, after feature encoding, we have $V_B = [v_1, v_2, \dots, v_B] \in \mathbb{R}^{B \times d}$ and $T_B = [t_1, t_2, \dots, t_B] \in \mathbb{R}^{B \times d}$. Next, the instance features V_B/T_B and the prototypes pt^v/pt^t are processed in a cross-attention decoder (CAD). This decoder enables interaction between instance features and prototypes, extracting identity-relevant information from instances to enrich the prototypes. There are N_e blocks in CAD, each featuring a multi-head cross-attention layer and a feed-forward network layer. For the cross-attention decoder, the prototypes pt^v/pt^t serve as *query*, while the instance features V_B/T_B are designated as *key* and *value*, which is formulated as follows:

$$p_{en,i}^v = CAD(pt^v, V_B, V_B), \quad p_{en,i}^t = CAD(pt^t, T_B, T_B), \quad (3)$$

where $p_{en,i}^v \in \mathbb{R}^d$ and $p_{en,i}^t \in \mathbb{R}^d$ represent the intra-modal instance-enriched visual and textual prototypes, respectively. This process enhances the prototypes using intra-modal instance features. Additionally, we extend this enrichment by incorporating inter-modal instance features, fostering the network to extract modality-shared identity information comprehensively and minimize the modal gap.

$$p_{eo,i}^v = CAD(pt^v, T_B, T_B), \quad p_{eo,i}^t = CAD(pt^t, V_B, V_B), \quad (4)$$

where $p_{eo,i}^v \in \mathbb{R}^d$ and $p_{eo,i}^t \in \mathbb{R}^d$ represent the inter-modal instance-enriched visual and textual prototypes, respectively.

3.5 Adaptive Prototype Aggregation

For both images and texts, we generate three distinct modality-specific prototypes: $p_{a,i}^m \in \mathbb{R}^d$, $p_{en,i}^m \in \mathbb{R}^d$, and $p_{eo,i}^m \in \mathbb{R}^d$, each containing different information for each identity L_i , where $m \in \{v, t\}$. To seamlessly integrate all available information, we introduce an Adaptive Prototype Aggregation (APA) module. This module effectively aggregates diverse prototypes to form a comprehensive identity-enriched prototype. Since pt_i^m is directly derived by CLIP, ensuring high-quality prototypes due to its robust semantic understanding capabilities. We designate pt_i^m as the prototype baseline for aggregation. The aggregation weights are determined based on the correlation of other prototypes with pt_i^m . This approach

enables the suppression of spurious identity prototype information in $p_{a,i}^m, p_{en,i}^m, p_{eo,i}^m$, while amplifying the correct ones during aggregation. The calculation of prototype correlation, serving as the aggregation weights for the three prototypes, is as follows:

$$w_{a,i}^m = pt_i^m (p_{a,i}^m)^T, \quad w_{en,i}^m = pt_i^m (p_{en,i}^m)^T, \quad w_{eo,i}^m = pt_i^m (p_{eo,i}^m)^T. \quad (5)$$

Then, we utilize the softmax function to normalize the weights and obtain the final identity-enriched prototype as

$$p_i^m = pt_i^m + \sum_k w_{k,i}^m \cdot p_{k,i}^m, \quad (6)$$

where $k \in \{a, en, eo\}$. Thus, for the entire training set, we can generate the final visual and textual prototype sets $p^v = [p_1^v, p_2^v, \dots, p_N^v] \in \mathbb{R}^{N \times d}$ and $p^t = [p_1^t, p_2^t, \dots, p_N^t] \in \mathbb{R}^{N \times d}$. Subsequently, we propagate the rich identity information encapsulated in the prototypes to each instance through prototype-to-instance contrastive loss to model identity-level matching for TIReID.

3.6 Training and Inference

The goal of Propot is to model both instance-level and identity-level matching for TIReID. To this end, we optimize Propot through cross-modal matching loss, cross-entropy loss, prototype-to-instance contrastive loss, and mask language modeling loss.

Given a batch of B image-text pairs $\{I_i, T_i\}_{i=1}^B$, we generate the global visual and textual features as $V_B = [v_1, v_2, \dots, v_B] \in \mathbb{R}^{B \times d}$ and $T_B = [t_1, t_2, \dots, t_B] \in \mathbb{R}^{B \times d}$. To align each image I_i and its annotated text T_i , we utilize the similarity distribution matching (SDM) [21] as the cross-modal matching loss to model instance-level matching between them.

$$\mathcal{L}_{sdm} = \mathcal{L}_{i2t} + \mathcal{L}_{t2i}, \quad (7)$$

$$\mathcal{L}_{i2t} = \frac{1}{B} \sum_{i=1}^B \sum_{j=1}^B p_{i,j} \log\left(\frac{p_{i,j}}{q_{i,j} + \epsilon}\right), \quad (8)$$

$$p_{i,j} = \frac{\exp(\text{sim}(v_i, t_j)/\tau)}{\sum_{k=1}^B \exp(\text{sim}(v_i, t_k)/\tau)}, \quad (9)$$

where $\text{sim}(\cdot)$ denotes the cosine similarity function, τ denotes the temperature factor to control the distribution peaks, and ϵ is a small number to avoid numerical problems. $q_{i,j}$ denotes the true matching probability. α indicates the margin. \mathcal{L}_{t2i} can be obtained by exchanging v and t in Eqs. 8 and 9. Moreover, to ensure the discriminability of features v and t , we calculate cross-entropy loss \mathcal{L}_{id} on them to classify them into corresponding identity labels.

Through the prototype learning process described above, we generate two identity-rich prototypes p_i^v and p_i^t for each identity L_i . To effectively diffuse the rich identity information encapsulated in the prototypes to instances of the same identity, we employ a prototype-to-instance contrastive loss, denoted as \mathcal{L}_{p2i} . This loss operates in tandem with the cross-modal matching loss, collectively contributing to the modeling of identity-level matching.

$$\mathcal{L}_{p2i} = \sum_{i=1}^N \mathcal{L}_{p2v}(L_i) + \mathcal{L}_{p2t}(L_i), \quad (10)$$

$$\mathcal{L}_{p2v}(L_i) = -\frac{1}{|P(L_i)|} \sum_{p \in P(L_i)} \frac{\exp(\text{sim}(v_p, p_i^v)/\tau)}{\sum_{k=1}^B \exp(\text{sim}(v_j, p_i^v)/\tau)}, \quad (11)$$

$$\mathcal{L}_{p2i}(L_i) = -\frac{1}{|P(L_i)|} \sum_{p \in P(L_i)} \frac{\exp(\text{sim}(t_p, p_i^t)/\tau)}{\sum_{k=1}^B \exp(\text{sim}(t_j, p_i^t)/\tau)}, \quad (12)$$

where $P(L_i)$ represents a set of instance indices of identity L_i , and $|P(L_i)|$ denotes the cardinality of $P(L_i)$. To further improve performance, we follow [21] to introduce a mask language modeling task \mathcal{L}_{mlm} to model fine-grained matching between modalities.

Propot is a single-stage and end-to-end trainable framework, and the overall objective function \mathcal{L} for training is as follows:

$$\mathcal{L} = \mathcal{L}_{sdm} + \mathcal{L}_{id} + \lambda_1 \mathcal{L}_{p2i} + \lambda_2 \mathcal{L}_{mlm}, \quad (13)$$

where λ_1 and λ_2 balance the contribution of different loss terms.

4 EXPERIMENTS

4.1 Experiment Settings

Datasets and Metrics: The evaluations are conducted on three datasets for TIReID. **CUHK-PEDES** [33] has 40,206 images and 80,412 descriptions of 13,003 persons. Each image has 2 descriptions, each with an average length of 23 words. The training set has 34,054 images and 68,108 descriptions of 11,003 persons, the validation set includes 3,078 images and 6,156 descriptions of 1,000 persons, and the testing set involves 3,074 images and 6,148 descriptions of 1,000 persons. **ICFG-PEDES** [9] comprises 54,522 image-text pairs of 4,102 persons, with descriptions averaging 37 words in length. We utilize 34,674 pairs of 3,102 persons for training and reserving the remaining 1,000 persons for evaluation. **RSTPReid** [80] includes 20,505 images of 4,101 persons, each annotated with 2 descriptions, with descriptions averaging 23 words in length. There are 3,701 persons in the training set, 200 persons in the validation set, and 200 persons in the testing set. For performance evaluation, we employ the Rank- k matching accuracy ($R@k$, $k=1, 5, 10$) and the mean Average Precision (mAP).

Implementation Details: For input images, we uniformly resize them to 384×128 and augment them with random horizontal flipping, random crop with padding, and random erasing. For input texts, the length of the token sequence is unified to 77 and augmented by randomly masking out some tokens with a 15% probability [8]. Propot’s visual encoder is initialized with the CLIP-ViT-B/16 version of CLIP, where the dimension d of global visual and textual features is 512. The SAE and CAD consist of $N_a = 1$ and $N_e = 3$ blocks, respectively, each with 8 heads. The length K of the learnable prompt vector in the DPP module is set to 4. The temperature factor τ is 0.02. The loss balance factors are set to $\lambda_1 = 0.2$ and $\lambda_2 = 1.0$. Model training utilizes the Adam optimizer with a weight decay factor of $4e-5$. Initial learning rates are $1e-5$ for the visual/textual encoder and $1e-4$ for other network modules. We employ a cosine learning rate decay strategy, stopping training at 60 epochs. The learning rate linearly decays by a factor of 0.1 within the first 10% of the training epochs for warmup. All experiments are implemented in PyTorch library, and models are trained with a batch size of 64 on a single RTX3090 24GB GPU.

4.2 Comparisons with State-of-the-art Models

In this section, we compare our Propot with current state-of-the-art (SOTA) approaches on all three TIReID benchmarks. The compared methods are categorized into two sections: methods (w/o CLIP) based on single-modal pre-training models (ResNet [17], ViT [12],

Table 1: Performance comparison with state-of-the-art methods on CUHK-PEDES. R@1, R@5, and R@10 are listed. ‘-’ denotes that no reported result is available.

Methods	Pre	Ref	R@1	R@5	R@10	mAP
C ₂ A ₂ [43]		MM’22	64.82	83.54	89.77	-
FedSH [39]		TMM’23	60.87	80.82	87.61	-
PBSL [50]		MM’23	65.32	83.81	89.26	-
BEAT [41]		MM’23	65.61	83.45	89.57	-
MANet [69]		TNNLS’23	65.64	83.01	88.78	-
ASAMN [44]		TIP’23	65.66	84.53	90.21	-
LCR ² S [67]		MM’23	67.36	84.19	89.62	59.24
TransTPS [2]		TMM’23	68.23	86.37	91.65	-
MGCN [15]		TMM’23	69.40	87.07	90.82	62.49
CFine [68]		TIP’23	69.57	85.93	91.15	-
VLP-TPS [59]		arXiv’23	70.16	86.10	90.98	66.32
VGSG [18]		TIP’23	71.38	86.75	91.86	-
IRRA [21]		CVPR’23	73.38	89.93	93.71	66.13
TCB [74]		MM’23	74.45	90.07	<u>94.66</u>	64.12
DCEL [34]		MM’23	75.02	<u>90.89</u>	94.52	-
SAL [14]		MMM’24	69.14	85.90	90.81	-
EESSO [64]		IVC’24	69.57	85.65	90.71	-
PD [35]		arXiv’24	71.59	87.95	92.45	65.03
CFAM [81]		CVPR’24	72.87	88.61	92.87	64.92
MACF [52]		IJCV’24	73.33	88.57	93.02	-
TBPS-CLIP [3]		AAAI’24	73.54	88.19	92.35	65.38
UMSA [76]		AAAI’24	74.25	89.83	93.58	66.15
LSPM [26]		TMM’24	74.38	89.51	93.42	67.74
IRLT [36]		AAAI’24	74.46	90.19	94.01	-
MDRL [71]		AAAI’24	74.56	92.56	96.30	-
FSRL [58]		ICMR’24	74.65	89.77	94.03	<u>67.49</u>
Ours		MM’24	<u>74.89</u>	89.90	94.17	67.12

BERT [8]) and methods (w/ CLIP) based on multi-modal pre-training CLIP [48] models. Propot falls under the second section.

The performance comparison with SOTA methods on **CUHK-PEDES** is summarized in Table 1. The proposed Propot framework demonstrates competitive performance at all metrics and outperforms all compared methods except [34], achieving remarkable R@1, R@5, and R@10 accuracies of 74.89%, 89.90% and 94.17%, respectively. While our R@1 accuracy is slightly lower (-0.13%) compared to the optimal method DCEL [34], it is essential to note that DCEL introduces both mask language modeling and global-local semantic alignment to mine fine-grained matching. Additionally, as observed in Table 4#6, even without a local matching module, Propot achieves a noteworthy 74.37% R@1 accuracy, surpassing most compared methods. Table 2 reports the comparative results on **ICFG-PEDES**. Our Propot establishes a new SOTA performance on this dataset, with R@1, R@5, and R@10 accuracy scores of 65.12%, 81.57%, and 86.97%, respectively. The comparative analysis with SOTA methods on **RSTPReid** is summarized in Table 3. Propot demonstrates commendable performance, achieving competitive results over recent SOTA methods, specifically attaining 61.83%, 83.45%, and 89.70% on R@1, R@5, and R@10. Although our method achieves slightly lower performance (-0.08%) than the optimal method TBPS-CLIP [3], which incorporates CLIP into the TIReID task using various data augmentation and training tricks. In contrast, our approach uses only basic data augmentation without additional tricks. In summary, propot achieves superior performance on all three benchmarks.

Table 2: Performance comparison with state-of-the-art methods on ICFG-PEDES. R@1, R@5, and R@10 are listed. '-' denotes that no reported result is available.

Methods	Pre	Ref	R@1	R@5	R@10	mAP
FedSH [39]	w/o CLIP	TMM'23	55.01	72.75	79.48	-
ASAMN [44]		TIP'23	57.09	76.33	82.84	-
PBSL [50]		MM'23	57.84	75.46	82.15	-
LCR ² S [67]		MM'23	57.93	76.08	82.40	38.21
BEAT [41]		MM'23	58.25	75.92	81.96	-
MANet [69]		TNNLS'23	59.44	76.80	82.75	-
MGCN [15]		TMM'23	60.20	76.75	83.90	37.56
VLP-TPS [59]	w/ CLIP	arXiv'23	60.64	75.97	81.76	42.78
CFine [68]		TIP'23	60.83	76.55	82.42	-
TCB [74]		MM'23	61.60	76.33	81.90	44.31
VGSg [18]		TIP'23	63.05	78.43	84.36	-
IRRA [21]		CVPR'23	63.46	80.25	85.82	38.06
DCEL [34]		MM'23	64.88	81.34	86.72	-
EESSO [64]		IVC'24	60.84	77.89	83.53	-
PD [35]		arXiv'24	60.93	77.96	84.11	36.44
CFAM [81]		CVPR'24	62.17	79.57	85.32	39.42
SAL [14]		MMM'24	62.77	78.64	84.21	-
MACF [52]		IJCV'24	62.95	79.93	85.04	-
TBPS-CLIP [3]		AAAI'24	65.05	80.34	85.47	39.83
LSPM [26]		TMM'24	64.40	79.96	85.41	42.60
IRLT [36]	AAAI'24	64.72	81.35	86.31	-	
FSRL [58]	ICMR'24	64.01	80.42	85.86	39.64	
Ours		MM'24	65.12	81.57	86.97	42.93

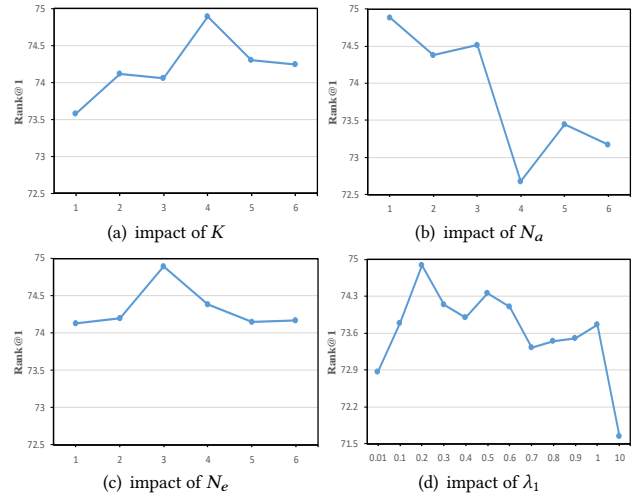
4.3 Ablation Studies

Contributions of Proposed Components: In Table 4, we assess the contribution of each module of Propot. Baseline solely includes visual and textual encoders initialized by CLIP, which is trained using SDM and cross-entropy loss. Baseline achieves an R@1 accuracy of 72.73%. Introducing our prototype learning process based on Baseline, aimed at modeling identity-level matching, yields several key observations. Firstly, using only the initial prototype (IniPt) generated by CLIP to supervise identity-level matching leads to distinct performance improvements (+0.35% R@1 improvement over Baseline), affirming the importance of identity-level matching. Secondly, incorporating the DPP module to update the initial prototype results in a 1.38% R@1 accuracy improvement over Baseline, demonstrating the effective adaptation of the initial prototype to TIReID. Thirdly, when the IPP module is employed to update the prototype, whether conditioned on intra-modal or inter-modal instances, substantial performance enhancements are observed (+1.1% or +0.92% R@1 improvement over Baseline). The performance is further elevated when both IPP modules are utilized concurrently, underscoring the IPP module's capacity to enrich the prototype with instance information. Fourthly, the collaborative use of DPP and IPP modules further enhances the R@1 accuracy to 74.37%, surpassing most SOTA methods in Table 1. Finally, incorporating the local matching module gets the best performance for Propot. Additionally, Tables 4 show the computational complexity of Propot, the prototype prompting process requires only light computational overhead (20% of total parameters and an additional 10 GFLOPs), and it is removed during inference.

Impact of contextual vector length K in DPP: To facilitate the initial prototype adapt to the TIReID task, we introduce a set of learnable contextual prompt vectors for each prototype in the DPP module. The length K of these vectors is a crucial parameter

Table 3: Performance comparison with state-of-the-art methods on RSTPReid. R@1, R@5, and R@10 are listed. '-' denotes that no reported result is available.

Methods	Pre	Ref	R@1	R@5	R@10	mAP
LBUL [62]	w/o CLIP	MM'22	45.55	68.20	77.85	-
ACSA [19]		TMM'22	48.40	71.85	81.45	-
C ₂ A ₂ [43]		MM'22	51.55	76.75	85.15	-
PBSL [50]		MM'23	47.80	71.40	79.90	-
BEAT [41]		MM'23	48.10	73.10	81.30	-
MGCN [15]		TMM'23	52.95	75.30	84.04	41.74
LCR ² S [67]		MM'23	54.95	76.65	84.70	40.92
TransTPS [2]	TMM'23	56.05	78.65	86.75	-	
CFine [68]	w/ CLIP	TIP'23	50.55	72.50	81.60	-
VLP-TPS [59]		arXiv'23	50.65	72.45	81.20	43.11
IRRA [21]		CVPR'23	60.20	81.30	88.20	47.17
DCEL [34]		MM'23	61.35	83.95	90.45	-
EESSO [64]		IVC'24	53.15	74.80	83.55	-
PD [35]		arXiv'24	56.65	77.40	84.70	45.27
CFAM [81]		CVPR'24	59.40	81.35	88.50	49.50
TBPS-CLIP [3]		AAAI'24	61.95	83.55	88.75	48.26
IRLT [36]		AAAI'24	61.49	82.26	89.23	-
FSRL [58]		ICMR'24	60.20	81.40	88.60	47.38
Ours		MM'24	61.87	83.63	89.70	47.82


Figure 3: Effects of four hyper-parameters on CUHK-PEDES, including contextual vector length K , the block number N_a , N_e , and loss weight λ_1 .

affecting the prototype's adaptation. To explore the impact of different vector lengths, we vary K from 1 to 6 and report the results in Figure 3 (a). The observed trend indicates that larger values of K result in better performance, as they provide more contextual parameters to capture TIReID task information. Notably, when K equals 4, the performance reaches a peak of 74.89%. However, excessively large K values may introduce redundant information, leading to overfitting and increased computational costs. Hence, we set K to 4 to strike a balance between performance and efficiency.

Influence of N_a , N_e : The parameters N_a and N_e determine the number of blocks in SAE and CAD, respectively. Their impact on performance is shown in Figure 3 (b) and (c). Regarding N_a , we observe a notable performance drop when its value exceeds 3. Too many SAE parameters might impede the learning of contextual prompt vectors. Therefore, we set N_a to 1, which yields the optimal

Table 4: Ablation study on different components of our Propot on CUHK-PEDES.

No.	Methods	IniPt	DPP	IPP		MLM	R@1	R@5	R@10	Params	FLOPs
				Intra	Inter						
0#	Baseline						72.73	88.91	93.01	155.26M	20.266
1#	+IniP	✓					73.08	88.97	93.19	155.26M	20.278
2#	+DPP	✓	✓				74.11	89.46	93.57	203.48M	25.704
3#	+IPP (Intra)	✓		✓			73.83	89.21	93.53	158.41M	23.058
4#	+IPP (Inter)	✓			✓		73.65	89.42	93.69	158.41M	23.058
5#	+IPP	✓		✓	✓		74.03	89.47	93.66	158.41M	25.838
6#	+DPP+IPP	✓	✓	✓	✓		74.37	89.59	93.88	206.64M	31.264
7#	+DPP+IPP+MLM	✓	✓	✓	✓	✓	74.89	89.90	94.17	245.91M	37.353

Table 5: Ablation study of prototype aggregation schemes on CUHK-PEDES.

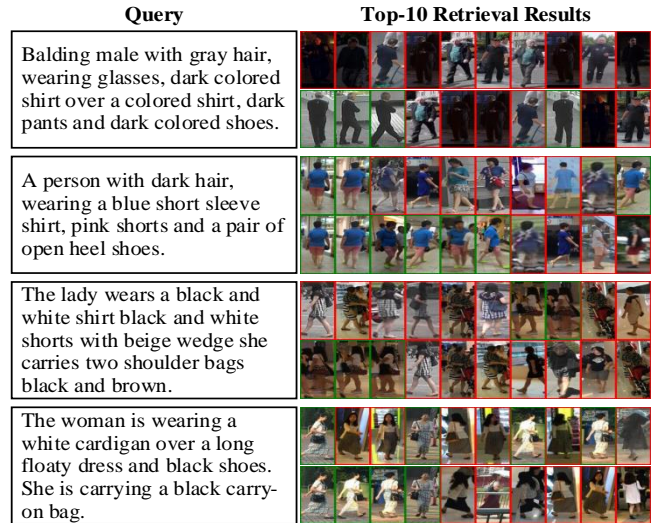
Method	Rank-1	Rank-5	Rank-10
Sum	74.30	89.86	93.84
Average	74.29	89.39	93.34
MLP	73.51	89.56	93.76
Parameter	74.19	89.10	93.18
APA (Ours)	74.89	89.90	94.17

result. Conversely, our model shows less sensitivity to N_e , with its curve displaying a relatively stable trend. However, excessively large N_e values would introduce unnecessary parameters, leading to increased computational costs. Hence, we set N_e to 3 to achieve superior performance while maintaining efficiency.

Impact of weight λ_1 in the objective function: λ_1 determines the strength of identity-level matching. To assess its effect, we conduct experiments by varying λ_1 from 0.01 to 10, as depicted in Figure 3 (d). Results indicate that increasing λ_1 leads to gradual performance improvement, peaking at 0.2. However, further increase in λ_1 results in performance decline, collapsing when λ_1 reaches 10. This pattern occurs because too small λ_1 fails to effectively spread identity information to instances, making identity-level matching ineffective. Conversely, excessively large λ_1 disrupts instance-level matching by over-diffusing identity information. Therefore, we set λ_1 to 0.2 in the experiment to balance instance-level and identity-level matching.

Different Prototype Aggregation Schemes: We introduced the APA module to adaptively combine multiple prototypes generated by different modules. To demonstrate its effectiveness, we compared APA with several common aggregation schemes: (1) summing prototypes, (2) averaging prototypes, (3) using a multi-layer perceptron (MLP) to assign weights to prototypes, and (4) learning weights for prototypes simultaneously with the network. Table 5 summarizes the comparison results. From the analysis, we draw the following conclusions: Aggregation methods with learnable weights perform worse than those without. This is because adding parameters makes optimization more difficult and uncertain for the network. Simple summation or averaging of prototypes yields superior performance, highlighting the effectiveness of our approach. The strength of our aggregation method lies in its use of the CLIP-generated initial prototype as a baseline for combining other prototypes adaptively. The quality of the initial prototype is guaranteed by CLIP’s strong semantic understanding capabilities.

Qualitative Results: To showcase the effectiveness of Propot, we present retrieval results in Figure 4. For each query text, Figure 4 displays the top-10 gallery images retrieved by both the baseline and

**Figure 4: Retrieval result comparisons of Baseline (the 1st row) and Propot (the 2nd row) on CUHK-PEDES. The matched and mismatched person images are marked with green and red rectangles, respectively.**

Propot. Baseline solely focuses on instance-level matching, whereas Propot incorporates prototype prompting to include identity-level matching. The examples show that Propot excels where the baseline struggles, ensuring images with the same identity as the given query text rank high. This highlights the importance of identity-level matching, with Propot outperforming by modeling both instance-level and identity-level matching simultaneously.

5 CONCLUSION

In this study, to model identity-level matching for TIReID, we present Propot, a conceptually simple framework for identity-enriched prototype learning. The framework follows the ‘initialize, adapt, enrich, then aggregate’ pipeline. Initially, we generate robust initial prototypes using CLIP. Then, we employ the Domain-conditional Prototypical Prompting (DPP) module to prompt and adapt the initial prototypes to the TIReID task. To ensure prototype diversity, the Instance-conditional Prototypical Prompting (DPP) is devised, enriching the prototypes with both intra-modal and inter-modal instances. Finally, we use an adaptive prototype aggregation module to effectively combine multiple prototypes and diffuse their rich identity information to instances, thereby enabling identity-level

matching. Through extensive experiments conducted on three popular benchmarks, we demonstrate the superiority and effectiveness of the proposed Propot framework.

ACKNOWLEDGMENTS

This work was supported in part by the National Natural Science Foundation of China under Grant 61925204 and Grant 62172212, the Natural Science Foundation of Jiangsu Province under Grant BK20230031.

REFERENCES

- [1] Yang Bai, Min Cao, Daming Gao, Ziqiang Cao, Chen Chen, Zhenfeng Fan, Liqiang Nie, and Min Zhang. 2023. Towards unified text-based person retrieval: A large-scale multi-attribute and language search benchmark. In *ACM International Conference on Multimedia, MM*.
- [2] Liping Bao, Longhui Wei, Wengang Zhou, Lin Liu, Lingxi Xie, Houqiang Li, and Qi Tian. 2024. Multi-Granularity Matching Transformer for Text-Based Person Search. *IEEE Transactions on Multimedia* 26 (2024), 4281–4293.
- [3] Min Cao, Yang Bai, Ziyin Zeng, Mang Ye, and Min Zhang. 2024. An Empirical Study of CLIP for Text-based Person Search. In *AAAI Conference on Artificial Intelligence, AAAI*.
- [4] Yucheng Chen, Rui Huang, Hong Chang, Chuanqi Tan, Tao Xue, and Bingpeng Ma. 2021. Cross-Modal Knowledge Adaptation for Language-Based Person Search. *IEEE Transactions on Image Processing* 30 (2021), 4057–4069.
- [5] Yen-Chun Chen, Linjie Li, Licheng Yu, Ahmed El Kholy, Faisal Ahmed, Zhe Gan, Yu Cheng, and Jingjing Liu. 2020. UNITER: UNiversal Image-Text Representation Learning. In *European Conference on Computer Vision, ECCV*.
- [6] Yuhao Chen, Guoqing Zhang, Yujiang Lu, Zhenxing Wang, and Yuhui Zheng. 2022. TIPCB: A simple but effective part-based convolutional baseline for text-based person search. *Neurocomputing* 494 (2022), 171–181.
- [7] Jia Deng, Wei Dong, Richard Socher, Li-Jia Li, Kai Li, and Li Fei-Fei. 2009. ImageNet: A large-scale hierarchical image database. In *IEEE Computer Society Conference on Computer Vision and Pattern Recognition, CVPR*.
- [8] Jacob Devlin, Ming-Wei Chang, Kenton Lee, and Kristina Toutanova. 2019. BERT: Pre-training of Deep Bidirectional Transformers for Language Understanding. In *The North American Chapter of the Association for Computational Linguistics, NAACL*.
- [9] Zefeng Ding, Changxing Ding, Zhiyin Shao, and Dacheng Tao. 2021. Semantically Self-Aligned Network for Text-to-Image Part-aware Person Re-identification. *arXiv preprint arXiv:2107.12666* (2021).
- [10] Neng Dong, Shuanglin Yan, Hao Tang, Jinhui Tang, and Liyan Zhang. 2024. Multi-view information integration and propagation for occluded person re-identification. *Information Fusion* 104 (2024), 102201.
- [11] Neng Dong, Liyan Zhang, Shuanglin Yan, Hao Tang, and Jinhui Tang. 2024. Erasing, Transforming, and Noising Defense Network for Occluded Person Re-identification. *IEEE Transactions on Circuits and Systems for Video Technology* 34, 6 (2024), 4458–4472.
- [12] Alexey Dosovitskiy, Lucas Beyer, Alexander Kolesnikov, Dirk Weissenborn, Xiuhua Zhai, Thomas Unterthiner, Mostafa Dehghani, Matthias Minderer, Georg Heigold, Sylvain Gelly, Jakob Uszkoreit, and Neil Houlsby. 2021. An Image is Worth 16x16 Words: Transformers for Image Recognition at Scale. In *International Conference on Learning Representations, ICLR*.
- [13] Han Fang, Pengfei Xiong, Luhui Xu, and Yu Chen. 2021. CLIP2Video: Mastering Video-Text Retrieval via Image CLIP. *arXiv preprint arXiv:2106.11097* (2021).
- [14] Wenjun Gan, Jiawei Liu, Yangchun Zhu, Yong Wu, Guozhi Zhao, and Zhengjun Zha. 2024. Cross-Modal Semantic Alignment Learning for Text-Based Person Search. In *International Conference on Multimedia Modeling, MMM*.
- [15] Guang Han, Min Lin, Ziyang Li, Haitao Zhao, and Sam Kwong. 2024. Text-to-Image Person Re-Identification Based on Multimodal Graph Convolutional Network. *IEEE Transactions on Multimedia* 26 (2024), 6025–6036.
- [16] Xiao Han, Sen He, Li Zhang, and Tao Xiang. 2021. Text-Based Person Search with Limited Data. In *British Machine Vision Conference, BMVC*.
- [17] Kaiming He, Xiangyu Zhang, Shaoqing Ren, and Jian Sun. 2016. Deep Residual Learning for Image Recognition. In *IEEE Conference on Computer Vision and Pattern Recognition, CVPR*.
- [18] Shuting He, Hao Luo, Wei Jiang, Xudong Jiang, and Henghui Ding. 2024. VGSG: Vision-Guided Semantic-Group Network for Text-Based Person Search. *IEEE Transactions on Image Processing* 33 (2024), 163–176.
- [19] Zhong Ji, Junhua Hu, Deyin Liu, Lin Yuanbo Wu, and Ye Zhao. 2023. Asymmetric Cross-Scale Alignment for Text-Based Person Search. *IEEE Transactions on Multimedia* 25 (2023), 7699–7709.
- [20] Chao Jia, Yinfei Yang, Ye Xia, Yi-Ting Chen, Zarana Parekh, Hieu Pham, Quoc V. Le, Yun-Hsuan Sung, Zhen Li, and Tom Duerig. 2021. Scaling Up Visual and Vision-Language Representation Learning With Noisy Text Supervision. In *International Conference on Machine Learning, ICML*.
- [21] Ding Jiang and Mang Ye. 2023. Cross-Modal Implicit Relation Reasoning and Aligning for Text-to-Image Person Retrieval. In *IEEE Conference on Computer Vision and Pattern Recognition, CVPR*.
- [22] Zhengbao Jiang, Frank F Xu, Jun Araki, and Graham Neubig. 2020. How can we know what language models know? *Transactions of the Association for Computational Linguistics* 8 (2020), 423–438.
- [23] Ya Jing, Chenyang Si, Junbo Wang, Wei Wang, Liang Wang, and Tieniu Tan. 2020. Pose-guided multi-granularity attention network for text-based person search. In *AAAI Conference on Artificial Intelligence, AAAI*.
- [24] Chen Ju, Tengda Han, Kunhao Zheng, Ya Zhang, and Weidi Xie. 2022. Prompting visual-language models for efficient video understanding. In *European Conference on Computer Vision, ECCV*.
- [25] Huaifeng Li, Shuanglin Yan, Zhengtao Yu, and Dapeng Tao. 2019. Attribute-identity embedding and self-supervised learning for scalable person re-identification. *IEEE Transactions on Circuits and Systems for Video Technology* 30, 10 (2019), 3472–3485.
- [26] Jiayi Li, Min Jiang, Jun Kong, Xuefeng Tao, and Xi Luo. 2024. Learning Semantic Polymorphic Mapping for Text-Based Person Retrieval. *IEEE Transactions on Multimedia* (2024), 1–14. <https://doi.org/10.1109/TMM.2024.3410129>
- [27] Junnan Li, Ramprasaath Selvaraju, Akhilesh Gotmare, Shafiq Joty, Caiming Xiong, and Steven Chu Hong Hoi. 2021. Align before fuse: Vision and language representation learning with momentum distillation. *Advances in neural information processing systems, NeurIPS* (2021).
- [28] Liunian Harold Li, Mark Yatskar, Da Yin, Cho-Jui Hsieh, and Kai-Wei Chang. 2019. VisualBERT: A Simple and Performant Baseline for Vision and Language. *arXiv preprint arXiv:1908.03557* (2019).
- [29] Shiping Li, Min Cao, and Min Zhang. 2022. Learning Semantic-Aligned Feature Representation for Text-Based Person Search. In *IEEE International Conference on Acoustics, Speech and Signal Processing, ICASSP*.
- [30] Shuang Li, Jiaxu Leng, Ji Gan, Mengjingcheng Mo, and Xinbo Gao. 2023. Shape-centered Representation Learning for Visible-Infrared Person Re-identification. *arXiv preprint arXiv:2310.17952* (2023).
- [31] Shuang Li, Fan Li, Jinxing Li, Huaifeng Li, Bob Zhang, Dapeng Tao, and Xinbo Gao. 2023. Logical Relation Inference and Multiview Information Interaction for Domain Adaptation Person Re-Identification. *IEEE Transactions on Neural Networks and Learning Systems* (2023), 1–13. <https://doi.org/10.1109/TNNLS.2023.3281504>
- [32] Siyuan Li, Li Sun, and Qingli Li. 2023. Clip-reid: Exploiting vision-language model for image re-identification without concrete text labels. In *AAAI Conference on Artificial Intelligence, AAAI*.
- [33] Shuang Li, Tong Xiao, Hongsheng Li, Bolei Zhou, Dayu Yue, and Xiaogang Wang. 2017. Person Search with Natural Language Description. In *IEEE Conference on Computer Vision and Pattern Recognition, CVPR*.
- [34] Shenshen Li, Xing Xu, Yang Yang, Fumin Shen, Yijun Mo, Yujie Li, and Heng Tao Shen. 2023. DCEL: Deep Cross-modal Evidential Learning for Text-Based Person Retrieval. In *ACM International Conference on Multimedia, MM*.
- [35] Weihao Li, Lei Tan, Pingyang Dai, and Yan Zhang. 2024. Prompt Decoupling for Text-to-Image Person Re-identification. *arXiv preprint arXiv:2401.02173* (2024).
- [36] Yu Liu, Guihe Qin, Haipeng Chen, Zhiyong Cheng, and Xun Yang. 2024. Causality-Inspired Invariant Representation Learning for Text-Based Person Retrieval. In *AAAI Conference on Artificial Intelligence, AAAI*.
- [37] Jiasen Lu, Dhruv Batra, Devi Parikh, and Stefan Lee. 2019. ViLBERT: Pretraining Task-Agnostic Visiolinguistic Representations for Vision-and-Language Tasks. In *Advances in Neural Information Processing Systems, NeurIPS*.
- [38] Huaishao Luo, Lei Ji, Ming Zhong, Yang Chen, Wen Lei, Nan Duan, and Tianrui Li. 2022. CLIP4Clip: An Empirical Study of CLIP for End to End Video Clip Retrieval. *Neurocomputing* 508 (2022), 293–304.
- [39] Wentao Ma, Xinyi Wu, Shan Zhao, Tongqing Zhou, Dan Guo, Lichuan Gu, Zhiping Cai, and Meng Wang. 2024. FedSH: Towards Privacy-Preserving Text-Based Person Re-Identification. *IEEE Transactions on Multimedia* 26 (2024), 5065–5077.
- [40] Yiwei Ma, Jiayi Ji, Xiaoshuai Sun, Yiyi Zhou, and Rongrong Ji. 2023. Towards local visual modeling for image captioning. *Pattern Recognition* 138 (2023), 109420.
- [41] Yiwei Ma, Xiaoshuai Sun, Jiayi Ji, Guanman Jiang, Weilin Zhuang, and Rongrong Ji. 2023. Beat: Bi-directional One-to-Many Embedding Alignment for Text-based Person Retrieval. In *ACM International Conference on Multimedia, MM*.
- [42] Yiwei Ma, Guohai Xu, Xiaoshuai Sun, Ming Yan, Ji Zhang, and Rongrong Ji. 2022. X-clip: End-to-end multi-grained contrastive learning for video-text retrieval. In *ACM International Conference on Multimedia, MM*.
- [43] Kai Niu, Linjiang Huang, Yan Huang, Peng Wang, Liang Wang, and Yanning Zhang. 2022. Cross-modal Co-occurrence Attributes Alignments for Person Search by Language. In *ACM International Conference on Multimedia, MM*.
- [44] Kai Niu, Tao Huang, Linjiang Huang, Liang Wang, and Yanning Zhang. 2023. Improving Inconspicuous Attributes Modeling for Person Search by Language. *IEEE Transactions on Image Processing* 32 (2023), 3429–3441.
- [45] Kai Niu, Yan Huang, Wanli Ouyang, and Liang Wang. 2020. Improving description-based person re-identification by multi-granularity image-text alignments. *IEEE Transactions on Image Processing* 29 (2020), 5542–5556.

- [46] Yang Qin, Yingke Chen, Dezhong Peng, Xi Peng, Joey Tianyi Zhou, and Peng Hu. 2024. Noisy-Correspondence Learning for Text-to-Image Person Re-identification. In *IEEE Conference on Computer Vision and Pattern Recognition, CVPR*.
- [47] Yang Qin, Dezhong Peng, Xi Peng, Xu Wang, and Peng Hu. 2022. Deep Evidential Learning with Noisy Correspondence for Cross-modal Retrieval. In *ACM International Conference on Multimedia, MM*.
- [48] Alec Radford, Jong Wook Kim, Chris Hallacy, Aditya Ramesh, Gabriel Goh, Sandhini Agarwal, Girish Sastry, Amanda Askell, Pamela Mishkin, Jack Clark, Gretchen Krueger, and Ilya Sutskever. 2021. Learning Transferable Visual Models From Natural Language Supervision. In *International Conference on Machine Learning, ICML*.
- [49] Zhiyin Shao, Xinyu Zhang, Meng Fang, Zhifeng Lin, Jian Wang, and Changxing Ding. 2022. Learning Granularity-Unified Representations for Text-to-Image Person Re-identification. In *ACM International Conference on Multimedia, MM*.
- [50] Fei Shen, Xiangbo Shu, Xiaoyu Du, and Jinhui Tang. 2023. Pedestrian-specific bipartite-aware similarity learning for text-based person retrieval. In *ACM International Conference on Multimedia, MM*.
- [51] Taylor Shin, Yasaman Razeghi, Robert L. Logan IV, Eric Wallace, and Sameer Singh. 2020. AutoPrompt: Eliciting Knowledge from Language Models with Automatically Generated Prompts. In *Conference on Empirical Methods in Natural Language Processing, EMNLP*.
- [52] Mengyang Sun, Wei Suo, Peng Wang, Kai Niu, Le Liu, Guosheng Lin, Yanning Zhang, and Qi Wu. 2024. An Adaptive Correlation Filtering Method for Text-Based Person Search. *International Journal of Computer Vision* (2024), 1–16. <https://doi.org/10.1007/s11263-024-02094-8>
- [53] Hao Tang, Zechao Li, Zhimao Peng, and Jinhui Tang. 2020. BlockMix: Meta Regularization and Self-Calibrated Inference for Metric-Based Meta-Learning. In *ACM International Conference on Multimedia, MM*.
- [54] Hao Tang, Jun Liu, Shuanglin Yan, Rui Yan, Zechao Li, and Jinhui Tang. 2023. M3Net: Multi-view Encoding, Matching, and Fusion for Few-shot Fine-grained Action Recognition. In *ACM International Conference on Multimedia, MM*.
- [55] Hao Tang, Chengcheng Yuan, Zechao Li, and Jinhui Tang. 2022. Learning attention-guided pyramidal features for few-shot fine-grained recognition. *Pattern Recognition* 130 (2022), 108792. <https://doi.org/10.1016/j.patcog.2022.108792>
- [56] Kaiyang Zhou, Jingkang Yang, Chen Change Loy, and Ziwei Liu. 2022. Conditional prompt learning for vision-language models. In *IEEE Conference on Computer Vision and Pattern Recognition, CVPR*.
- [57] Chengji Wang, Zhiming Luo, Yaojin Lin, and Shaozi Li. 2021. Text-based Person Search via Multi-Granularity Embedding Learning. In *International Joint Conference on Artificial Intelligence, IJCAI*.
- [58] Di Wang, Feng Yan, Yifeng Wang, Lin Zhao, Xiao Liang, Haodi Zhong, and Ronghua Zhang. 2024. Fine-grained Semantics-aware Representation Learning for Text-based Person Retrieval. In *International Conference on Multimedia Retrieval, ICMR*.
- [59] Guanshuo Wang, Fufu Yu, Junjie Li, Qiong Jia, and Shouhong Ding. 2023. Exploiting the Textual Potential from Vision-Language Pre-training for Text-based Person Search. *arXiv preprint arXiv:2303.04497* (2023).
- [60] Wenhui Wang, Hangbo Bao, Li Dong, Johan Bjorck, Zhiliang Peng, Qiang Liu, Kriti Aggarwal, Owais Khan Mohammed, Saksham Singhal, Subhojit Som, et al. 2023. Image as a Foreign Language: BEiT Pretraining for Vision and Vision-Language Tasks. In *IEEE Conference on Computer Vision and Pattern Recognition, CVPR*.
- [61] Zhaoping Wang, Yu Lu, Qiang Li, Xunqiang Tao, Yandong Guo, Mingming Gong, and Tongliang Liu. 2022. CRIS: CLIP-Driven Referring Image Segmentation. In *IEEE Conference on Computer Vision and Pattern Recognition, CVPR*.
- [62] Zijie Wang, Aichun Zhu, Jingyi Xue, Xili Wan, Chao Liu, Tian Wang, and Yifeng Li. 2022. Look Before You Leap: Improving Text-based Person Retrieval by Learning A Consistent Cross-modal Common Manifold. In *ACM International Conference on Multimedia, MM*.
- [63] Yushuang Wu, Zizheng Yan, Xiaoguang Han, Guanbin Li, Changqing Zou, and Shuguang Cui. 2021. LapsCore: Language-Guided Person Search via Color Reasoning. In *International Conference on Computer Vision, ICCV*.
- [64] Jingyi Xue, Zijie Wang, Guan-Nan Dong, and Aichun Zhu. 2024. EESSO: Exploiting Extreme and Smooth Signals via Omni-frequency learning for Text-based Person Retrieval. *Image and Vision Computing* 142 (2024), 104912.
- [65] Rui Yan, Lingxi Xie, Xiangbo Shu, Liyan Zhang, and Jinhui Tang. 2023. Progressive Instance-Aware Feature Learning for Compositional Action Recognition. *IEEE Transactions on Pattern Analysis and Machine Intelligence* 45, 8 (2023), 10317–10330.
- [66] Rui Yan, Lingxi Xie, Jinhui Tang, Xiangbo Shu, and Qi Tian. 2023. HiGCIN: Hierarchical Graph-Based Cross Inference Network for Group Activity Recognition. *IEEE Transactions on Pattern Analysis and Machine Intelligence* 45, 6 (2023), 6955–6968.
- [67] Shuanglin Yan, Neng Dong, Jun Liu, Liyan Zhang, and Jinhui Tang. 2023. Learning Comprehensive Representations with Richer Self for Text-to-Image Person Re-Identification. In *ACM international conference on Multimedia, MM*.
- [68] Shuanglin Yan, Neng Dong, Liyan Zhang, and Jinhui Tang. 2023. CLIP-Driven Fine-Grained Text-Image Person Re-Identification. *IEEE Transactions on Image Processing* 32 (2023), 6032–6046.
- [69] Shuanglin Yan, Hao Tang, Liyan Zhang, and Jinhui Tang. 2023. Image-Specific Information Suppression and Implicit Local Alignment for Text-based Person Search. *IEEE Transactions on Neural Networks and Learning Systems* (2023), 1–14. <https://doi.org/10.1109/TNNLS.2023.3310118>
- [70] Shuanglin Yan, Yafei Zhang, Minghong Xie, Dacheng Zhang, and Zhengtao Yu. 2022. Cross-domain person re-identification with pose-invariant feature decomposition and hypergraph structure alignment. *Neurocomputing* 467 (2022), 229–241.
- [71] Fan Yang, Wei Li, Menglong Yang, Binbin Liang, and Jianwei Zhang. 2024. Multi-Modal Disordered Representation Learning Network for Description-Based Person Search. In *AAAI Conference on Artificial Intelligence, AAAI*.
- [72] Shuyi Yang, Yanan Zhou, Zhedong Zheng, Yaxiong Wang, Li Zhu, and Yujiao Wu. 2023. Rasa: Relation and sensitivity aware representation learning for text-based person search. In *International Joint Conference on Artificial Intelligence, IJCAI*.
- [73] Lewei Yao, Runhui Huang, Lu Hou, Guansong Lu, Minzhe Niu, Hang Xu, Xiaodan Liang, Zhenguo Li, Xin Jiang, and Chunjing Xu. 2022. FILIP: Fine-grained Interactive Language-Image Pre-Training. In *International Conference on Learning Representations, ICLR*.
- [74] Xianghao Zang, Wei Gao, Ge Li, Han Fang, Chao Ban, Zhongjiang He, and Hao Sun. 2023. A Baseline Investigation: Transformer-based Cross-view Baseline for Text-based Person Search. In *ACM International Conference on Multimedia, MM*.
- [75] Ying Zhang and Huchuan Lu. 2018. Deep cross-modal projection learning for image-text matching. In *European Conference on Computer Vision, ECCV*.
- [76] Zhiwei Zhao, Bin Liu, Yan Lu, Qi Chu, and Nenghai Yu. 2024. Unifying Multi-Modal Uncertainty Modeling and Semantic Alignment for Text-to-Image Person Re-identification. In *AAAI Conference on Artificial Intelligence, AAAI*.
- [77] Kecheng Zheng, Wu Liu, Jiawei Liu, Zheng-Jun Zha, and Tao Mei. 2020. Hierarchical gumbel attention network for text-based person search. In *ACM International Conference on Multimedia, MM*.
- [78] Zhedong Zheng, Liang Zheng, Michael Garrett, Yi Yang, Mingliang Xu, and Yi-Dong Shen. 2020. Dual-path convolutional image-text embeddings with instance loss. *ACM Transactions on Multimedia Computing, Communications, and Applications* 16, 2 (2020), 51:1–51:23.
- [79] Kaiyang Zhou, Jingkang Yang, Chen Change Loy, and Ziwei Liu. 2022. Learning to prompt for vision-language models. *International Journal of Computer Vision* 130, 9 (2022), 2337–2348.
- [80] Aichun Zhu, Zijie Wang, Yifeng Li, Xili Wan, Jing Jin, Tian Wang, Fangqiang Hu, and Gang Hua. 2021. DSSL: Deep Surroundings-person Separation Learning for Text-based Person Retrieval. In *ACM International Conference on Multimedia, MM*.
- [81] Jialong Zuo, Hanyu Zhou, Ying Nie, Feng Zhang, Tianyu Guo, Nong Sang, Yunhe Wang, and Changxin Gao. 2024. UFineBench: Towards Text-based Person Retrieval with Ultra-fine Granularity. In *IEEE Conference on Computer Vision and Pattern Recognition, CVPR*.